

Ultra-high stacks of InGaAs/GaAs quantum dots for high efficiency solar cells†

Takeyoshi Sugaya,^{aa} Osamu Numakami,^{ab} Ryuji Oshima,^a Shigenori Furue,^a Hironori Komaki,^a Takeru Amano,^a Koji Matsubara,^a Yoshinobu Okano^b and Shigeru Niki^a

Received 10th June 2011, Accepted 12th January 2012

DOI: 10.1039/c2ee01930b

We report ultra-high stacked InGaAs/GaAs quantum dot (QD) solar cells fabricated by the intermittent deposition of $In_{0.4}Ga_{0.6}As$ under an As_2 source using molecular beam epitaxy. We obtain a 400-stack $In_{0.4}Ga_{0.6}As$ QD structure without using a strain balancing technique, in which the total number of QDs reaches $2 \times 10^{13} \text{ cm}^{-2}$. Photoluminescence and cross-sectional scanning transmission electron microscope measurements indicate that the $In_{0.4}Ga_{0.6}As$ QD structure exhibits no degradation in crystal quality, no dislocations and no crystal defects even after the stacking of 400 QD layers. The external quantum efficiency and the short-circuit current density of multi-stacked $In_{0.4}Ga_{0.6}As$ QD solar cells increase as the number of stacked layers is increased to 150. Such ultra-high stacks and good cell performance have not been reported for QD solar cells using other material systems. The performance of the ultra-high stacked QD solar cells indicates that InGaAs QDs are suitable for use in high efficiency solar cells requiring thick QD layers for sufficient light absorption.

Introduction

Intermediate-band solar cells with quantum dot (QD) superlattice structures have been expected as candidates for third generation solar cells.¹ QD superlattice structures are inserted in the p–n junction of the barrier materials to realize intermediate-band solar cells. Self-assembled QD structures grown by

molecular beam epitaxy have recently attracted much attention as a medium for QD superlattices. To realize intermediate-band solar cells, we need highly stacked QD superlattice structures with a miniband that are uniform and periodically distributed in all three dimensions.² Although the InAs/GaAs QD material system has been widely studied, the crystal quality of InAs/GaAs QDs degrades as the number of QD layers increases owing to the buildup of internal strain. Therefore, the InAs/GaAs QD solar cell performance also degrades as the number of QD layers increases.³ To overcome these problems, a strain balancing growth technique has been demonstrated with GaNAs⁴ or GaP⁵ buffer layers for InAs/GaAs material systems. However, the external quantum efficiency (EQE) decreased greatly in a 100-stack InAs/GaNAs solar cell,⁶ and there are few reports on the ultra-high stacking of more than 300 QD layers.⁷

^aNational Institute of Advanced Industrial Science and Technology (AIST), 1-1-1 Umezono, Tsukuba 305-8568, Japan. E-mail: t.sugaya@aist.go.jp; Fax: +81 29 861 5615; Tel: +81 29 861 5466

^bTokyo City University, 1-28-1 Tamazutsumi, Setagaya-ku, Tokyo 158-8557, Japan

† This article was submitted as part of a collection highlighting research from the Advanced inorganic materials and concepts for photovoltaics symposium, at the 2011 E-MRS Bilateral Energy Conference.

Broader context

The increase in the demand for renewable energy means that we can expect the cost of photovoltaic technologies to be greatly reduced and to provide super-high conversion efficiency. Quantum dot (QD) solar cells (intermediate-band solar cells) have recently been studied extensively and are expected to provide a high conversion efficiency of over 60%. To realize such high efficiency solar cells, we need highly stacked QD superlattice structures that are uniform and distributed periodically in all three dimensions. In this paper, we report high-quality and ultra-high stacks of 400-layer $In_{0.4}Ga_{0.6}As$ QD structures that we achieved without using a strain balancing growth technique in molecular beam epitaxy. Moreover, 150-stack $In_{0.4}Ga_{0.6}As$ QD solar cells offer good cell performance, which has not been reported for any other material system. Ultra-high stacked QD structures grown without using a strain balancing technique are very attractive for further investigation of QD solar cells. We can use various materials to fabricate other QD material systems that are capable of realizing ideal intermediate-band solar cells if we do not need strain balancing techniques to grow the ultra-high stacked QD structures.

InGaAs QDs are alternative candidates for stacked structures because of their small lattice mismatch with GaAs substrates. We have reported the successful stacking of 100-layer $\text{In}_{0.4}\text{Ga}_{0.6}\text{As}$ QDs without using any strain balancing technique. The structure was fabricated by the intermittent deposition of $\text{In}_{0.4}\text{Ga}_{0.6}\text{As}$ layers and by using an As_2 source, and as a result there was no degradation in crystal quality.^{8,9} Multi-stacked $\text{In}_{0.4}\text{Ga}_{0.6}\text{As}$ QD solar cells have good cell characteristics even though no strain balancing methods are employed.¹⁰ In this paper, we report high quality and ultra-high stacks of 400-layer $\text{In}_{0.4}\text{Ga}_{0.6}\text{As}$ QD structures that we achieved without using a strain balancing growth technique. Moreover, 150-stack $\text{In}_{0.4}\text{Ga}_{0.6}\text{As}$ QD solar cells offer good cell performance, which has not been reported for any other material system.

Experimental

We grew 200, 300 and 400-stack $\text{In}_{0.4}\text{Ga}_{0.6}\text{As}$ QD layers on a Si-doped GaAs (001) substrate using an As_2 source.^{11,12} The $\text{In}_{0.4}\text{Ga}_{0.6}\text{As}$ QD and GaAs buffer layers were 2 and 20 nm thick, respectively. We employed a growth interruption of 20 s after growing the InGaAs QD layers for 200 and 300-stack structures, which meant the intermittent deposition of $\text{In}_{0.4}\text{Ga}_{0.6}\text{As}$. For 400-stack QD layers, a growth interruption of 5 s was employed to reduce the total growth time. The growth temperature was 520 °C. The As_2 pressure and the growth rate of the $\text{In}_{0.4}\text{Ga}_{0.6}\text{As}$ QDs were 4.5×10^{-6} Torr and 1.0 $\mu\text{m h}^{-1}$, respectively. We employed photoluminescence (PL), scanning electron microscopy (SEM), and cross-sectional scanning transmission electron microscopy (STEM) observations to measure the optical properties, surface and cross-sectional structures of the QDs, respectively. The PL measurements were performed using an Ar^+ laser and a Ge photodetector at 11 K. The excitation intensity was $\sim 10 \text{ W cm}^{-2}$. We carried out high resolution X-ray diffraction (HR-XRD) to determine both the strained state and periodicity of 400-stack QD structures.

The sample structure of the solar cell devices is shown in Fig. 1, in which i -layer multi-stacked QD structures were inserted in the GaAs p–n junction. The i -layer region consists of 10-, 20-, 30-, 50-, 100-, and 150-stack 2 nm $\text{In}_{0.4}\text{Ga}_{0.6}\text{As}$ QD structures. We employed a growth interruption of 10 s after growing the InGaAs QD layers for all device structures. The barrier layers between the QDs were 12 and 20 nm thick for the 150-stack and other structures, respectively. After the growth, the front electrode was formed using photolithography and a lift-off technique. Ti/Au and AuGe/Ni/Au were used for the front and rear electrodes, respectively. A 120 nm thick MgF_2 layer was employed as an

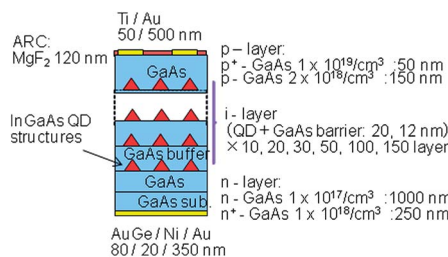


Fig. 1 Schematic layer structure of a multi-stacked InGaAs/GaAs QD solar cell grown on a GaAs (001) substrate.

anti-reflection coating (ARC). The EQE of the QD solar cells was measured directly under a constant photon irradiation of 10^{14} cm^{-2} . The performance of the QD solar cells was also measured under standard conditions of AM1.5G, 100 mW cm^{-2} , and 25 °C.

Results and discussion

Fig. 2(a)–(c) show SEM micrographs of the surface plane on top of the 200-, 300-, and 400-stack structures. The surface density of the 200- and 300-stack QD structures was $6.4 \times 10^{10} \text{ cm}^{-2}$ and that of the 400-stack structure was $4.4 \times 10^{10} \text{ cm}^{-2}$. The diameters of the 200- and 300-stack QDs were 20–30 nm, and those of 400-stack QDs were 15–25 nm. These results are due to the difference in the growth interruption time, because the QDs become larger during the growth interruption. The ultra-high stacked structure had a good surface morphology even after the stacking of 400 QD layers. The area densities in the 300 and 400-stack $\text{In}_{0.4}\text{Ga}_{0.6}\text{As}$ QD layers were as high as $1.9 \times 10^{13} \text{ cm}^{-2}$ and $1.8 \times 10^{13} \text{ cm}^{-2}$, respectively.

Fig. 3(a)–(c) show enlarged cross-sectional STEM images of the top, middle and bottom portions, respectively, of 300-stack $\text{In}_{0.4}\text{Ga}_{0.6}\text{As}$ QD layers. $\text{In}_{0.4}\text{Ga}_{0.6}\text{As}$ QDs can be seen with a diameter of $\sim 30 \text{ nm}$ and a height of $\sim 7 \text{ nm}$. The QDs were aligned at an angle of 55–65° to the (001) surface. No dislocations were generated after stacking 300 layers, even though no strain balancing was employed during the growth.

Fig. 4 shows the PL spectra of 200-, 300-, and 400-stack $\text{In}_{0.4}\text{Ga}_{0.6}\text{As}$ QD layers at 11 K. The PL spectra of 20- and 30-stack QD structures are also shown as a reference. The PL intensities of the 200-, 300- and 400-stack QDs were higher than those of the 20- and 30-stack QDs, which have high crystal qualities.⁸ Because all the 400-layer QDs were not excited by using an Ar^+ laser ($\lambda = 514.5 \text{ nm}$), the PL spectra originated mainly from the upper portions of the stacked structures and

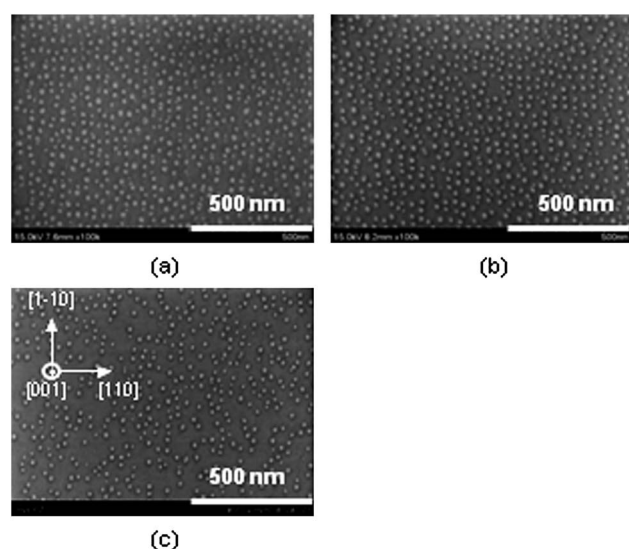


Fig. 2 SEM micrographs of the surface plane on top of (a) 200, (b) 300, (c) 400-stack $\text{In}_{0.4}\text{Ga}_{0.6}\text{As}$ QD structures. The ultra-high stacked structures have good surface morphologies even after the stacking of 300 or 400 QD layers.

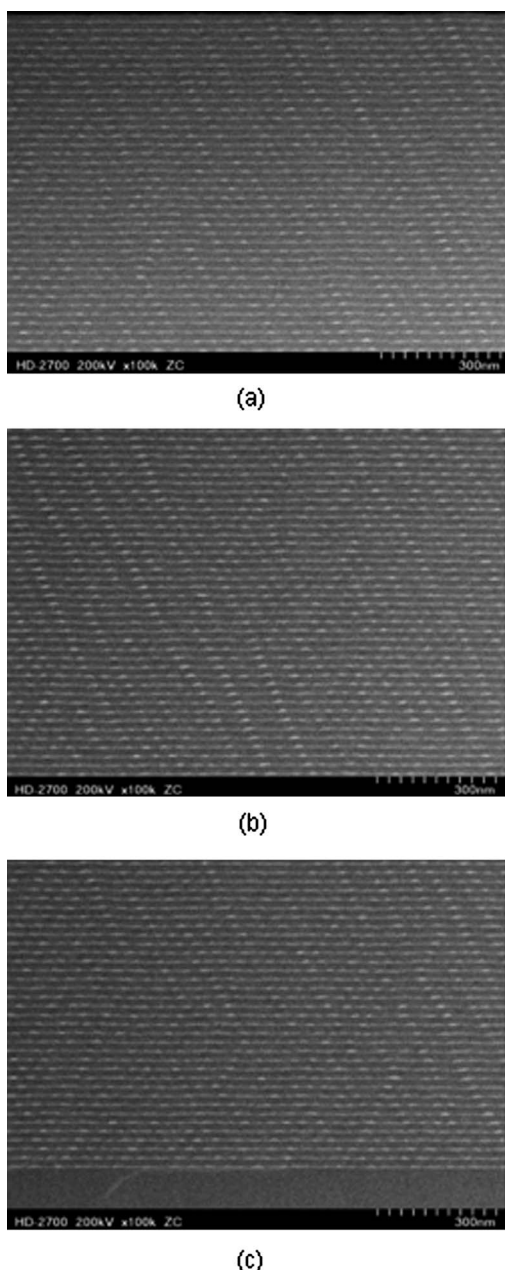


Fig. 3 Enlarged cross-sectional STEM images of (a) top, (b) middle and (c) bottom portions of 300-stack $\text{In}_{0.4}\text{Ga}_{0.6}\text{As}$ QD layers. No dislocations were generated after the stacking of 300 layers, even though no strain balancing was employed during the growth.

reflect their crystal qualities. The above results indicate the growth of high-quality and ultra-high stacks of $\text{In}_{0.4}\text{Ga}_{0.6}\text{As}$ QD structures even after the stacking of 400 layers without using any special strain balancing methods. The thicknesses of the 300 and 400-stack $\text{In}_{0.4}\text{Ga}_{0.6}\text{As}/\text{GaAs}$ QD structures are thought to be still lower than the critical values.

The PL wavelength for the 200- and 300-stack QD layers was longer than that for 400-stack QD layers. The difference in the PL wavelength was attributed to the different QD sizes that result from the different growth interruption times. The 400-stack QDs were smaller than the 200- and 300-stack QDs because of the reduced growth interruption time, as shown in

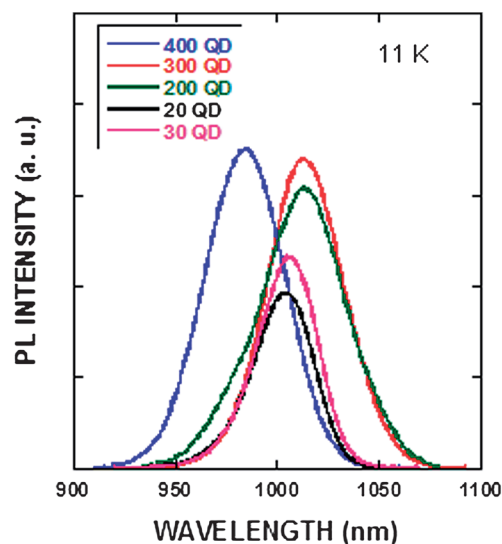


Fig. 4 PL spectra of 200-, 300-, and 400-stack $\text{In}_{0.4}\text{Ga}_{0.6}\text{As}$ QD layers at 11 K. The PL spectra of 20- and 30-stack QD structures are also shown as a reference.

Fig. 1. The PL wavelength for the 200- and 300-stack QD layers was also longer than that for the 20- and 30-stack structures because of their different QD heights. As shown in Fig. 2, the QDs were 7 nm high for the 200- and 300-stack QD structures, and 5 nm high for the 20- and 30-stack QD structures.⁸

Fig. 5 shows reciprocal space mapping (RSM) measurements around asymmetric (244) reflection in HRXRD. The clear satellite peaks arrangement in the RSM was observed along the growth direction Q_y with the peak S for the GaAs substrate, which suggested that no lattice relaxation occurred during the stacking. The appearance of satellite peaks along Q_y such as F_{+5y} and F_{-6y} in the figure indicates that the placement of QDs is highly ordered to the growth direction. We calculated the mean period Λ between the QD layers along the (001) direction by using the following equation,

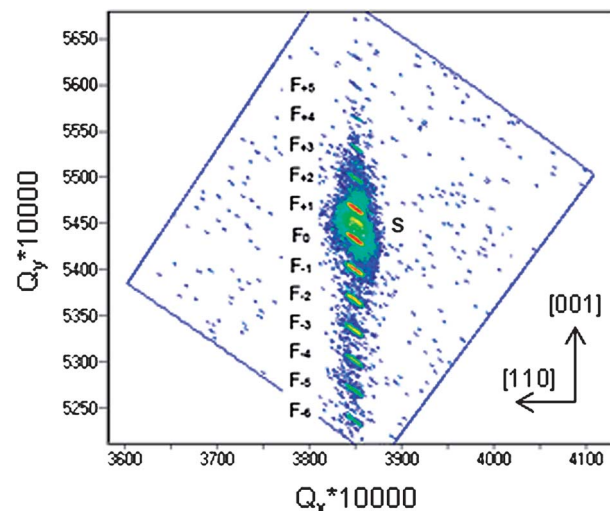


Fig. 5 RSM of diffracted X-ray intensity around the (244) reflection measured for 400-stack $\text{In}_{0.4}\text{Ga}_{0.6}\text{As}$ quantum dots. Q_x and Q_y are along the [110] and [001] azimuth, respectively.

$$\Lambda = (n_i - n_j)\lambda/2(\sin \omega_i - \sin \omega_j), \quad (1)$$

where n_i and n_j are the degrees and ω_i and ω_j are the Bragg angles of the i^{th} and j^{th} order satellite peaks, respectively. λ is the wavelength of X-ray ($\text{CuK}\alpha_1 \approx 0.15456 \text{ nm}$). The mean spacing between the dots was $\Lambda = 22.8 \text{ nm}$, which was in good agreement with the growth thickness of 22 nm. The average lattice mismatch between the InGaAs QD structures and the GaAs substrate is estimated to be 0.183% from the difference between the 0th-order peak F_0 and the peak S . We believe that the thickness of 400-stack InGaAs QD structure is lower than the critical value because of such a small lattice mismatch.

Fig. 6 shows the EQE spectra of the multi-stacked $\text{In}_{0.4}\text{Ga}_{0.6}\text{As}$ QD solar cells and a GaAs reference cell. The EQEs of the 10-, 20-, 30-, 50-, 100- and 150-stack $\text{In}_{0.4}\text{Ga}_{0.6}\text{As}$ QD solar cells are indicated. The QD diameter in all devices is the same because we employed the same growth interruption time of 10 s. The EQE of the QD solar cells extended the photo-absorption spectra toward a wavelength longer than the GaAs band gap. The photo-absorption above 900 nm exhibited by the multi-stacked $\text{In}_{0.4}\text{Ga}_{0.6}\text{As}$ QD structures increased as the number of stacking layers increased. The peaks at around 920 nm are thought to be due to the photo-absorption of InGaAs wetting layers. The photo-absorption of InGaAs QDs is observed at around 1000 nm, which is mentioned in relation to the PL peaks in Fig. 4. Although the PL peak of InGaAs QDs is strong as shown in Fig. 4, the EQE is still small. This is due to the ineffective carrier extraction from the InGaAs QDs, which indicates that the QDs become recombination centers for the carriers.

The $\text{In}_{0.4}\text{Ga}_{0.6}\text{As}$ QD solar cells had a good EQE spectrum even after the stacking of 150 QD layers. However, the EQE spectrum became much worse for the 100-stack InAs/GaNAs QD solar cells.⁴ This indicates that InGaAs QDs are more suitable for highly stacked QD solar cell applications with high efficiency. A 150 QD solar cell has a 2.1 μm thick *i*-layer because the GaAs barrier layer is 12 nm thick. The photo-absorption spectrum for the 200 QD solar cell decreased because the *i*-layer thickness was too high at 2.8 μm . Reducing the barrier layer

thickness may improve the cell characteristics when stacking increased the number of QD layers.

Fig. 7 shows *I*–*V* curves of multi-stacked $\text{In}_{0.4}\text{Ga}_{0.6}\text{As}$ QD solar cells with various QD layers and a GaAs reference cell. *I*–*V* curves are shown for 10-, 20-, 30-, 50-, 100- and 150-stack QD solar cells. The parameters for each solar cell are given in Table 1. The short-circuit current density increased from $J_{\text{sc}} = 17.5$ to 23.6 mA cm^{-2} as the number of stacking layers increased, which we believe to be due to the increased EQE in the longer wavelength region. Although the open circuit voltage (V_{oc}) decreased as the number of stacking layers increased as shown in Fig. 7, the drop in V_{oc} was almost saturated above the 50 stacked layers. The conversion efficiency of the 50-stack QD solar cell was higher than that of the 30-stack QD cell. There have been few reports on high-quality and ultra-high stacked QD solar cells with over 100 layers. However, the $\text{In}_{0.4}\text{Ga}_{0.6}\text{As}$ QD solar cells have good cell characteristics even after the ultra-high stacking of 150 QD layers. Such good cell performance has not been reported for 100-stack QD solar cells using other materials.¹³

The V_{oc} value, shunt resistance and conversion efficiency decrease in thick layer QD solar cells as shown in Fig. 7. These phenomena are thought to be due to the recombination and inefficient collection of the carriers in the QD regions. We measured the dark saturation current densities of 10, 50, and 100-stack QD solar cells, which were $\sim 1 \times 10^7$, $\sim 4 \times 10^7$, and $\sim 2 \times 10^6 \text{ A cm}^{-2}$, respectively. The dark saturation current increased as the number of stacking layers increased. This is evidence of the increased recombination of the carriers in the depletion region. Various papers have reported a reduction in V_{oc} due to carrier recombination in QD solar cells,^{3–5} which is a problem that we must overcome.

The energy difference between the GaAs conduction band and the InGaAs QD state is about 0.2–0.3 eV. This value is extremely small for the additional photo-absorption from the solar spectrum, because there are few small energy photons in the solar spectrum. However, enhanced photo-absorption has been reported using the optical transition from the InAs QD state to the GaNAs conduction band in a Si-doped QD solar cell under

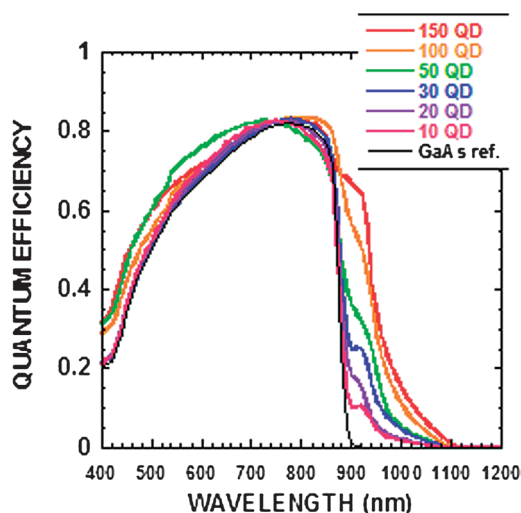


Fig. 6 EQE spectra of multi-stacked $\text{In}_{0.4}\text{Ga}_{0.6}\text{As}$ QD solar cells and a GaAs reference cell. The EQEs of the 10-, 20-, 30-, 50-, 100- and 150-stack $\text{In}_{0.4}\text{Ga}_{0.6}\text{As}$ QD solar cells are indicated.

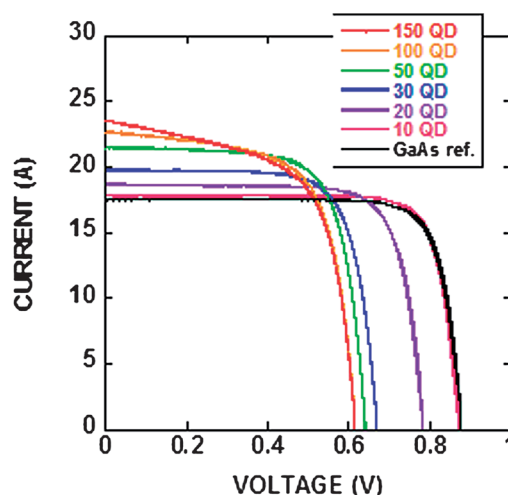


Fig. 7 *I*–*V* curves of multi-stacked $\text{In}_{0.4}\text{Ga}_{0.6}\text{As}$ QD solar cells with various QD layers and a GaAs reference cell. *I*–*V* curves are shown for 10-, 20-, 30-, 50-, 100- and 150-stack QD solar cells.

Table 1 Parameters of multi-stacked $\text{In}_{0.4}\text{Ga}_{0.6}\text{As}$ QD solar cells with various QD layers and a GaAs reference cell

QD layers	10	20	30	50	100	150	GaAs ref.
Efficiency (%)	12.4	11.3	9.8	10.0	9.4	9.2	12.4
V_{oc}/V	0.868	0.783	0.671	0.643	0.616	0.616	0.878
$J_{\text{sc}}/\text{mA cm}^{-2}$	17.7	18.7	19.7	21.5	22.7	23.6	17.5
FF	0.805	0.774	0.743	0.724	0.670	0.630	0.809

infrared light illumination conditions.¹⁴ This report indicates that the photocurrent can be increased by two-step photon absorption if we use appropriate doping and a suitable excitation source for the optical transition from the QD state to the conduction band. The reduced V_{oc} in the QD solar cells may also be improved by two-step photon absorption, because carrier recombination is reduced in the QD regions. We should realize a lower QD energy state in the GaAs band gap to obtain sufficient energy between the QD state and the conduction band to use the solar spectrum. We may need much smaller QDs in GaAs, or other material systems, to improve the characteristics of the QD solar cells. Moreover, concentrated sunlight may improve the reduced V_{oc} in the QD solar cells. We may be able to utilize enough infrared light illumination under concentrated sunlight conditions and thus improve the characteristics of the InGaAs QD solar cells.¹⁵ We need further studies to confirm the above discussions. Ultra-high stacked QD structures grown without using a strain balancing technique are very attractive for further investigation. We can use various materials to fabricate other QD material systems that are capable of realizing ideal intermediate-band solar cells if we do not need strain balancing techniques to grow the ultra-high stacked QD structures.

Conclusions

In conclusion, we have fabricated ultra-high stacked and high quality $\text{In}_{0.4}\text{Ga}_{0.6}\text{As}$ QD solar cells without using a strain balancing technique. PL, SEM, and STEM measurements indicate that the $\text{In}_{0.4}\text{Ga}_{0.6}\text{As}$ QD structure has good crystal quality and no dislocations even after the stacking of 400 QD layers. The EQE spectra and J_{sc} of the QD solar cells increase as the number of $\text{In}_{0.4}\text{Ga}_{0.6}\text{As}$ QD layers increases to 150. Such good cell performance has not been reported for ultra-high stacked QD solar cells with other material systems. The performance of the ultra-high stacked QD solar cells indicates that InGaAs QDs are suitable for high efficiency solar cell devices requiring thick QD layers for sufficient light absorption.

Acknowledgements

This work was partially supported by the New Energy and Industrial Technology Development Organization (NEDO) under the Ministry of Economy, Trade and Industry (METI).

Notes and references

- 1 A. Luque and A. Martí, Increasing the efficiency of ideal solar cells by photon induced transitions at intermediate levels, *Phys. Rev. Lett.*, 1997, **78**, 5014.
- 2 A. Luque, A. Martí, N. Lopez, E. Antolin, E. Canovas, C. Stanley, C. Farmer and P. Diaz, Operation of the intermediate band solar cell under nonideal space charge region conditions and half filling of the intermediate band, *J. Appl. Phys.*, 2006, **99**, 094503.
- 3 A. Martí, N. Lopez, E. Antolin, E. Canovas, A. Luque, C. Stanley, C. Farmer and P. Diaz, Emitter degradation in quantum dot intermediate band solar cells, *Appl. Phys. Lett.*, 2007, **90**, 233510.
- 4 R. Oshima, A. Takata and Y. Okada, Strain-compensated InAs/GaNAs quantum dots for use in high-efficiency solar cells, *Appl. Phys. Lett.*, 2008, **93**, 083111.
- 5 S. M. Hubbard, C. D. Cress, C. G. Bailey, R. P. Raffaelle, S. G. Bailey and D. M. Wilt, Effect of strain compensation on quantum dot enhanced GaAs solar cells, *Appl. Phys. Lett.*, 2008, **92**, 123512.
- 6 A. Takata, R. Oshima, Y. Shoji, K. Akahane and Y. Okada, Fabrication of 100 Layer-Stacked InAs/GaNAs Strain-Compensated Quantum Dots on GaAs (001) for Application to Intermediate Band Solar Cell, *Proceedings of 35th IEEE Photovoltaic Specialists Conference*, 2010, p. 001877.
- 7 K. Akahane, N. Yamamoto and T. Kawanishi, Fabrication of ultra-high-density InAs quantum dots using the strain-compensation technique, *Phys. Status Solidi A*, 2011, **208**, 425.
- 8 T. Sugaya, T. Amano, M. Mori, S. Niki and M. Kondo, Highly stacked and high quality quantum dots fabricated by intermittent deposition of InGaAs, *Jpn. J. Appl. Phys.*, 2010, **49**, 030211.
- 9 T. Sugaya, T. Amano, M. Mori and S. Niki, Highly stacked InGaAs quantum dot structures grown with two species of As, *J. Vac. Sci. Technol., B: Microelectron. Nanometer Struct.–Process., Meas., Phenom.*, 2010, **28**, C3C4.
- 10 T. Sugaya, Y. Kamikawa, S. Furue, T. Amano, M. Mori and S. Niki, Multi-stacked quantum dot solar cells fabricated by intermittent deposition of InGaAs, *Sol. Energy Mater. Sol. Cells*, 2011, **95**, 163.
- 11 T. Sugaya, T. Amano and K. Komori, Improved optical properties of InAs quantum dots grown with an As_2 source using molecular beam epitaxy, *J. Appl. Phys.*, 2006, **100**, 063107.
- 12 T. Sugaya, T. Amano and K. Komori, Suppressed bimodal size distribution of InAs quantum dots grown with an As_2 source using molecular beam epitaxy, *J. Appl. Phys.*, 2008, **104**, 083106.
- 13 S. M. Hubbard, C. Plourde, C. Bailey, Z. Bittner, M. Harris, T. Bald, M. Bennett, D. Forbes and R. Raffaelle, III-V Quantum Dot Enhanced Solar Cells, *Proceedings of 35th IEEE Photovoltaic Specialists Conference*, 2010, p. 001217.
- 14 Y. Okada, T. Morioka, K. Yoshida, R. Oshima, Y. Shoji, T. Inoue and T. Kita, Increase in photocurrent by optical transitions via intermediate quantum states in direct-doped InAs/GaNAs strain-compensated quantum dot solar cell, *J. Appl. Phys.*, 2011, **109**, 024301.
- 15 S. M. Hubbard, C. Bailey, R. Aguinaldo, S. Polly, D. Forbes and R. Raffaelle, Characterization of Quantum Dot Enhanced Solar Cells for Concentrator Photovoltaics, *Proceedings of 34th IEEE Photovoltaic Specialists Conference*, 2009, p. O131.